arXiv:1302.0646v2 [physics.flu-dyn] 26 Apr 2013

Tangling clustering instability for small particles in temperature stratified turbulence

T. Elperin[1],* N. Kleeorin[1,2],† M. Liberman[2,3],‡ and I. Rogachevskii[1,2§]
[1] *The Pearlstone Center for Aeronautical Engineering Studies, Department of Mechanical Engineering, Ben-Gurion University of the Negev, P. O. Box 653, Beer-Sheva 84105, Israel*
[2] *Nordita, KTH Royal Institute of Technology and Stockholm University, Roslagstullsbacken 23, 10691 Stockholm, Sweden*
[3] *Moscow Institute of Physics and Technology, Dolgoprudnyi, 141700, Russia*

(Dated: April 29, 2013)

We study particle clustering in a temperature stratified turbulence with small finite correlation time. It is shown that the temperature stratified turbulence strongly increases the degree of compressibility of particle velocity field. This results in the strong decrease of the threshold for the excitation of the tangling clustering instability even for small particles. The tangling clustering instability in the temperature stratified turbulence is essentially different from the inertial clustering instability that occurs in non-stratified isotropic and homogeneous turbulence. While the inertial clustering instability is caused by the centrifugal effect of the turbulent eddies, the mechanism of the tangling clustering instability is related to the temperature fluctuations generated by the tangling of the mean temperature gradient by the velocity fluctuations. Temperature fluctuations produce pressure fluctuations and cause particle clustering in regions with increased pressure fluctuations. It is shown that the growth rate of the tangling clustering instability is in $\sqrt{\mathrm{Re}}\,(\ell_0/L_T)^2/(3\mathrm{Ma})^4$ times larger than that of the inertial clustering instability, where Re is the Reynolds number, Ma is the Mach number, ℓ_0 is the integral turbulence scale and L_T is the characteristic scale of the mean temperature variations. It is found that depending on the parameters of the turbulence and the mean temperature gradient there is a preferential particle size at which the particle clustering due to the tangling clustering instability is more effective. The particle number density inside the cluster after the saturation of this instability can be in several orders of magnitude larger than the mean particle number density. It is also demonstrated that the evaporation of droplets drastically change the tangling clustering instability, e.g., it increases the instability threshold in the droplet radius. The tangling clustering instability is of a great importance, e.g., in atmospheric turbulence with temperature inversions.

PACS numbers: 47.27.tb, 47.27.T-, 47.55.Hd

I. INTRODUCTION

Formation of spatial inhomogeneities in the number density distribution of small inertial particles in a turbulent flow (also called particle clustering or preferential concentration) has attracted considerable attention in the past decades. [1–5] The enhanced number density of particles inside the cluster may affect the particle interactions, their dynamics and collisions, e.g. by enhancing the relative particle velocity and the rate of particle collisions and subsequent possible coalescence and/or separation of the particles. The dynamics of particle collisions is relevant to many phenomena in nature such as the raindrop formation and atmospheric aerosols dynamics [6–9], as well as to numerous industrial processes involving, e.g., spraying of liquid droplets in diesel and rocket engines [10]. Formation of clusters with enhanced number density of particles may increase the rate of particle collisions and coalescence [6, 8] and subsequently can significantly modify the size and velocity distributions of the droplets in the spray, which may, e.g., affect the combustor performance.

Clustering of inertial particles in a turbulent flow is caused by the centrifugal effect, which implies that the inertial particles are locally accumulated in regions between the turbulent eddies. These regions have a low vorticity, high strain rate, and maximum fluid pressure. Therefore, turbulent vortices act as small centrifuges that push heavy particles to the boundary regions between the eddies by the inertial forces creating concentration inhomogeneities. This effect is known as the inertia-induced particle clustering [11]. The inertial particle clustering in a turbulent flow has been studied analytically [12–20], numerically [21–28], and experimentally [2, 29–33].

There are two types of particle clustering. The first type is source clustering related to the source term in the equation for fluctuations of the particle number density. Most of analytical studies of preferential concentration are related to the source inertial clustering. Another type of particle clustering is associated with a spontaneous breakdown of their homogeneous spatial distribution due to the clustering instability. [15, 17] Although nature of the clustering instability is still not fully understood, the impact of the clustering instability on many processes, e.g. mixing, particle transport, etc., can be of great importance for different practical applications.

In the temperature stratified turbulence the particle clustering is affected by turbulent thermal diffusion.

---

* elperin@bgu.ac.il; http://www.bgu.ac.il/me/staff/tov
† nat@bgu.ac.il
‡ misha.liberman@gmail.com; http://michael-liberman.com/
§ gary@bgu.ac.il; http://www.bgu.ac.il/~gary

[34, 35] This phenomenon causes accumulation of the inertial particles in the vicinity of the mean temperature minimum and results in the formation of inhomogeneous mean particle number density distributions. Turbulent thermal diffusion is a purely collective phenomenon occurring in temperature stratified turbulence and resulting in the appearance of a non-zero mean effective velocity of particles in the direction opposite to the mean temperature gradient. A competition between the turbulent thermal diffusion and turbulent diffusion determines the conditions for the formation of large-scale particle concentrations in the vicinity of the mean temperature minimum. The phenomenon of turbulent thermal diffusion has been studied analytically [34–40], investigated by means of direct numerical simulations [41], and detected in the laboratory experiments in stably and unstably stratified turbulent flows [42, 43], and also observed in atmospheric turbulence. [40]

Particle clustering in the temperature stratified turbulence can be much more effective than the inertial particle clustering in isothermal turbulence. [44] The reason for this is that the mean temperature gradient in turbulent flow is a strong source of the temperature fluctuations which are correlated with the fluctuations of fluid velocity and pressure. The pressure fluctuations increase fluctuations of the particles number density and enhance the rate of formation of the particle clusters. Moreover, tangling of the mean gradient of particle number density (formed by the turbulent thermal diffusion) generates additional fluctuations of particle concentrations and contributes to the particle clustering.

The steady-state regime of the tangling clustering in temperature stratified turbulence without excitation of the tangling clustering instability (i.e., the regime of the source tangling clustering) has been recently studied experimentally and theoretically in Ref. 44. It was demonstrated that in the laboratory stratified turbulence the source tangling clustering is much more effective than a pure inertial clustering that has been observed in isothermal turbulence. In particular, in the experiments in oscillating grid isothermal turbulence in air without imposed mean temperature gradient, the inertial clustering is very weak for solid particles with the diameter $\approx 10\,\mu$m and Reynolds numbers based on turbulent length scale and rms velocity, $\mathrm{Re} = 250$. In the experiments [44] the correlation function for the inertial clustering in isothermal turbulence is much smaller than that for the tangling clustering in non-isothermal turbulence. The source tangling clustering was studied in Ref. 44 for inertial particles with small Stokes numbers and with the material density that is much larger than the fluid density.

The goal of the present paper is to conduct a comprehensive theoretical study of the tangling clustering instability in the temperature stratified turbulence. In this paper we show that in the presence of the imposed mean temperature gradient the tangling mechanism considerably enhances the rate of the clustering instability, and for small particles the tangling clustering instability in the presence of the imposed mean temperature gradient may result in the formation of small-scale inhomogeneities with the number density of particles exceeding the ambient average particle number density by several orders of magnitude.

The paper is organized as follows. The large-scale effects in particle transport in temperature stratified turbulence are discussed in Section II. The governing equations for analysis of instability are given in Section III. Solutions for the tangling clustering instability without (Section IV) and with the source term (Section V) are analyzed, and the instability growth rate and saturated value of the particle number density inside a cluster are determined. In Section VI we take into account an effect of droplet evaporation on tangling clustering instability. Finally, in Section VII we discuss the implications of the instability development and conclusions.

II. PARTICLES IN TEMPERATURE STRATIFIED TURBULENCE

A. Governing equations

Advection-diffusion equation for the number density $n_p(t, \boldsymbol{x})$ of inertial particles in a turbulent flow reads [45, 46]:

$$\frac{\partial n_p}{\partial t} + \boldsymbol{\nabla}\cdot(n_p\, \boldsymbol{v}) = D_m\, \Delta n_p, \tag{1}$$

where D_m is the coefficient of molecular (Brownian) diffusion, $\boldsymbol{v}(t, \boldsymbol{x})$ is the particle velocity field. We use a mean field approach in which the particle number density and velocity, the fluid temperature, density and pressure are decomposed into the mean and fluctuating parts, where the fluctuating parts have zero mean values. Averaging Eq. (1) over an ensemble of turbulent velocity fields we obtain an equation for the mean number density of particles:

$$\frac{\partial N}{\partial t} + \boldsymbol{\nabla}\cdot\, (N\, \boldsymbol{V}_p + \langle n\, \boldsymbol{v}\rangle) = D_m\, \Delta N, \tag{2}$$

where $N = \langle n_p\rangle$ is the mean particle number density, the angular brackets imply ensemble averaging, $\langle n\, \boldsymbol{v}\rangle$ is the turbulent flux of particles and $\boldsymbol{V}_p$ is the particle mean velocity. To obtain a closed mean-field equation one needs to determine the turbulent flux of particles. The equation for fluctuations of the particle number density, $n(t, \boldsymbol{x}) = n_p(t, \boldsymbol{x}) - N(t, \boldsymbol{x})$, then reads:

$$\frac{\partial n}{\partial t} + \boldsymbol{\nabla}\cdot(n\, \boldsymbol{v} - \langle n\, \boldsymbol{v}\rangle) - D_m\, \Delta n = -(\boldsymbol{v}\cdot\nabla)N - N\, \boldsymbol{\nabla}\cdot \boldsymbol{v}. \tag{3}$$

B. Turbulent thermal diffusion

Turbulent thermal diffusion results in formation of a nonzero gradient of the mean particle number density

$\boldsymbol{\nabla} N$ in temperature stratified turbulence. [34, 35] The physical mechanism of turbulent thermal diffusion is as follows. For the particles with the material density $\rho_m \gg \rho$, their velocity is determined by

$$\frac{d\boldsymbol{v}}{dt} = \frac{\boldsymbol{u} - \boldsymbol{v}}{\tau_s} + \boldsymbol{g}, \tag{4}$$

where $\boldsymbol{u}$ is the fluid velocity field, $\boldsymbol{g}$ is the acceleration of gravity, $\tau_s = m_p/6\pi\rho\,\nu a_p$ is the Stokes time for the small spherical particles of the radius a_p and mass m_p, ν is the kinematic viscosity, ρ is the mean fluid density. For small Stokes numbers, $\mathrm{St} = \tau_s/\tau_\eta \ll 1$, solution of Eq. (4) has the following form (see, e.g., Ref. 11):

$$\boldsymbol{v} = \boldsymbol{u} - \tau_s \left[\frac{\partial \boldsymbol{u}}{\partial t} + (\boldsymbol{u}\boldsymbol{\cdot}\boldsymbol{\nabla})\boldsymbol{u} - \boldsymbol{g}\right] + \mathrm{O}(\tau_s^2), \tag{5}$$

or introducing the dimensionless units, it can be written in dimensionless form:

$$\boldsymbol{v} = \boldsymbol{u} - \mathrm{St}\left[\frac{\partial \boldsymbol{u}}{\partial t} + (\boldsymbol{u}\boldsymbol{\cdot}\boldsymbol{\nabla})\boldsymbol{u} - \frac{\tau_\eta^2 \boldsymbol{g}}{\ell_\eta}\right] + \mathrm{O}(\mathrm{St}^2), \tag{6}$$

where distance is measured in the Kolmogorov viscous scale $\ell_\eta = \ell_0/\mathrm{Re}^{3/4}$ and the time is measured in the Kolmogorov time scale $\tau_\eta = \tau_0/\mathrm{Re}^{1/2}$. Here $\mathrm{Re} = \ell_0\, u_0/\nu$ is the fluid Reynolds numbers, u_0 is the characteristic turbulent velocity at the integral scale ℓ_0 of turbulent motions and $\tau_0 = \ell_0/u_0$. The terms in squared brackets in Eq. (5) describe the difference between the local fluid velocity and particle velocity arising due to the small but finite inertia of the particle. For the turbulent flow with low Mach numbers: $\boldsymbol{\nabla}\boldsymbol{\cdot}\boldsymbol{u} \approx -\rho^{-1}(\boldsymbol{u}\boldsymbol{\cdot}\boldsymbol{\nabla})\rho \neq 0$. The equation for $\boldsymbol{\nabla}\boldsymbol{\cdot}\boldsymbol{v}$ can be easily obtained from the equation (5) and the Navier-Stokes equation:

$$\boldsymbol{\nabla}\boldsymbol{\cdot}\boldsymbol{v} = \boldsymbol{\nabla}\boldsymbol{\cdot}\boldsymbol{u} - \tau_s\, \boldsymbol{\nabla}\boldsymbol{\cdot}\left(\frac{d\boldsymbol{u}}{dt}\right) + \mathrm{O}(\tau_s^2) = -\frac{1}{\rho}\,(\boldsymbol{u}\boldsymbol{\cdot}\boldsymbol{\nabla})\rho + \frac{\tau_s}{\rho}\,\boldsymbol{\nabla}^2 p + \mathrm{O}(\tau_s^2), \tag{7}$$

where p are the fluid pressure fluctuations. Due to inertia, particles inside the turbulent eddies drift out to the boundary regions between the eddies. These are regions with small velocity fluctuations and maximum pressure fluctuations. Consequently, particles are accumulated in the regions with the maximum pressure fluctuations of the turbulent fluid, i.e., $\boldsymbol{\nabla}\boldsymbol{\cdot}\boldsymbol{v} \propto (\tau_s/\rho)\,\boldsymbol{\nabla}^2 p \neq 0$ even for the incompressible fluid. For large Peclet numbers, when the molecular diffusion of particles in Eq. (1) can be neglected, we can estimate $\boldsymbol{\nabla}\boldsymbol{\cdot}\boldsymbol{v} \propto -dn_p/dt$. Therefore, inertial particles are accumulated (i.e., $dn_p/dt \propto -(\tau_s/\rho)\,\boldsymbol{\nabla}^2 p > 0$) in regions with maximum pressure of turbulent fluid, where $\boldsymbol{\nabla}^2 p < 0$. Similarly, there is an outflow of inertial particles from the regions with the minimum pressure of fluid. In case of homogeneous and isotropic turbulence a drift from regions with increased (decreased) concentration of particles by a turbulent flow of fluid is equiprobable in all directions.

On the contrary, in a temperature stratified turbulence, the turbulent heat flux $\langle \boldsymbol{u}\, \theta\rangle$ does not vanish. This implies that the fluctuations of fluid temperature, θ, and velocity are correlated, and, therefore, fluctuations of pressure are correlated with the fluctuations of velocity due to a non-zero turbulent heat flux, $\langle \boldsymbol{u}\, \theta\rangle \neq 0$. The increased pressure of the surrounding fluid is accompanied by the particles accumulation, and the direction of the mean flux of particles coincides with the direction of the heat flux of temperature towards the minimum of the mean temperature. [34, 44]

Equation for the mean number density N of particles reads:

$$\frac{\partial N}{\partial t} + \boldsymbol{\nabla}\boldsymbol{\cdot}\left[N\,(\boldsymbol{V} + \boldsymbol{W}_g) + \boldsymbol{F}^{(n)}\right] = D_m \triangle N, \tag{8}$$

where $\boldsymbol{V}_p = \boldsymbol{V} + \boldsymbol{W}_g$ is the mean particle velocity, $\boldsymbol{V}$ is the mean fluid velocity, $\boldsymbol{W}_g = \tau_s \boldsymbol{g}$ is the terminal fall velocity of particles, $D_m = k_B T/6\pi\rho\nu a_p$ is the coefficient of molecular (Brownian) diffusion, k_B is the Boltzman constant, T and ρ are the fluid mean temperature and density, respectively. The turbulent flux of particles, $\boldsymbol{F}^{(n)} = \langle n\, \boldsymbol{v}\rangle$, includes contributions of turbulent thermal diffusion and turbulent diffusion, i.e.,

$$\boldsymbol{F}^{(n)} = \boldsymbol{V}^{\rm eff}\, N - D_{_T}\, \boldsymbol{\nabla} N. \tag{9}$$

Here $D_{_T} \approx \ell_0\, u_0$ is the coefficient of turbulent diffusion, $\boldsymbol{V}^{\rm eff}$ is the effective pumping velocity caused by the turbulent thermal diffusion:

$$\boldsymbol{V}^{\rm eff} = -\tau\, \langle \boldsymbol{v}\, (\boldsymbol{\nabla}\boldsymbol{\cdot}\boldsymbol{v})\rangle, \tag{10}$$

where τ is the turbulent correlation time. Equation (10) for the effective velocity has been derived using different methods in Refs. 34, 36–40. The expression (10) can be obtained in a simple way using the dimensional consideration. Estimating the left hand side of Eq. (3) as

$$\frac{\partial n}{\partial t} + \boldsymbol{\nabla}\boldsymbol{\cdot}\left(n\, \boldsymbol{v} - \langle n\, \boldsymbol{v}\rangle\right) - D_m \boldsymbol{\nabla}^2 n \approx \frac{n}{\tau}, \tag{11}$$

we obtain an expression for the turbulent component n of the particle number density:

$$n \approx -\tau\, \boldsymbol{\nabla}\boldsymbol{\cdot}(N\, \boldsymbol{v}) = -\tau\, [N(\boldsymbol{\nabla}\boldsymbol{\cdot}\boldsymbol{v}) + (\boldsymbol{v}\boldsymbol{\cdot}\boldsymbol{\nabla})N]. \tag{12}$$

Therefore, the turbulent flux of particles $F_i^{(n)} = \langle v_i\, n\rangle$ is given by the following expression:

$$F_i^{(n)} = -N\, \tau\, \langle v_i\, (\boldsymbol{\nabla}\boldsymbol{\cdot}\boldsymbol{v})\rangle - \tau\, \langle v_i v_j\rangle \nabla_j N\ , \tag{13}$$

where the first term in the right hand side of Eq. (13) determines the turbulent flux of particles due to the turbulent thermal diffusion: $-N\, \tau\, \langle v_i\, (\boldsymbol{\nabla}\boldsymbol{\cdot}\boldsymbol{v})\rangle = V_i^{\rm eff}\, N$, and the second term in the right hand side of Eq. (13) describes the contribution of turbulent diffusion: $\tau\, \langle v_i v_j\rangle \nabla_j N = D_{_T}\, \nabla_i N$.

A detailed analysis [34, 44], using equation of state for an ideal gas with adiabatic index $c_{\rm p}/c_{\rm v}$ (the ratio of specific heats) and applying the identity $\tau_s = \rho\, W_g\, L_P/P$, yields the effective velocity in the following form:

$$\boldsymbol{V}^{\rm eff} = -\alpha\, D_{_T}\, \frac{\boldsymbol{\nabla} T}{T}, \tag{14}$$

where α is

$$\alpha = 1 + \frac{\mathrm{St}\,\ln(\mathrm{Re})}{\sqrt{\mathrm{Re}}\,\mathrm{Ma}^2}. \tag{15}$$

Here $L_P^{-1} = |\boldsymbol{\nabla} P|/P$, $\mathrm{Ma} = u_0/c_s$ is the Mach number and c_s is the sound speed. For gases and non-inertial particles $\alpha = 1$. A steady-state solution of Eq. (8) for $\boldsymbol{V} = 0$ is given by the following formula:

$$\frac{N(z)}{N_0} = \left[\frac{T(z)}{T_0}\right]^{-\frac{\alpha D_T}{D_m + D_T}} \exp\left[-\int_{z_0}^{z} \frac{W_{\rm g}}{D_m + D_T}\, dz'\right], \tag{16}$$

where $N_0 = N(z = z_0)$ and $T_0 = T(z = z_0)$ are the mean number density of particles and the mean fluid temperature, respectively, calculated at the boundary $z = z_0$. If there is a gradient of temperature in a vertical z direction, Eq. (16) implies that small particles are accumulated in the vicinity of the mean temperature minimum. This causes formation of large-scale inhomogeneous distributions of the mean particle number density.

III. GOVERNING EQUATIONS FOR ANALYSIS OF INSTABILITY

Let us study fluctuations of the particle number density. The equation for the two-point second-order correlation function of the particle number density, $\Phi(t, \boldsymbol{R}) = \langle n(t, \boldsymbol{x}) n(t, \boldsymbol{x} + \boldsymbol{R})\rangle$ was derived using Eq. (3) and path-integral approach in a turbulent compressible flow with a small finite correlation time (see Ref. 15):

$$\frac{\partial \Phi}{\partial t} = \left[B(\boldsymbol{R}) + 2\boldsymbol{U}^{(A)}(\boldsymbol{R}) \cdot \boldsymbol{\nabla} + \hat{D}_{ij}(\boldsymbol{R}) \nabla_i \nabla_j\right] \Phi(t, \boldsymbol{R}) + I(\boldsymbol{R}), \tag{17}$$

where $\boldsymbol{U}^{(A)}(\boldsymbol{R}) = (1/2)\left[\boldsymbol{U}(\boldsymbol{R}) - \boldsymbol{U}(-\boldsymbol{R})\right]$,

$$\hat{D}_{ij} = 2 D_m \delta_{ij} + D^{T}_{ij}(0) - D^{T}_{ij}(\boldsymbol{R}), \tag{18}$$

$$D^{T}_{ij}(\boldsymbol{R}) \approx 2 \int_0^\infty \langle v_i\left[0, \boldsymbol{\xi}(t, \boldsymbol{x}|0)\right] v_j\left[\tau, \boldsymbol{\xi}(t, \boldsymbol{x} + \boldsymbol{R}|\tau)\right]\rangle\, d\tau, \tag{19}$$

$$B(\boldsymbol{R}) \approx 2 \int_0^\infty \langle b\left[0, \boldsymbol{\xi}(t, \boldsymbol{x}|0)\right] b\left[\tau, \boldsymbol{\xi}(t, \boldsymbol{x} + \boldsymbol{R}|\tau)\right]\rangle\, d\tau, \tag{20}$$

$$U_i(\boldsymbol{R}) \approx -2 \int_0^\infty \langle v_i\left[0, \boldsymbol{\xi}(t, \boldsymbol{x}|0)\right] b\left[\tau, \boldsymbol{\xi}(t, \boldsymbol{x} + \boldsymbol{R}|\tau)\right]\rangle\, d\tau. \tag{21}$$

Here $b = \operatorname{div} \boldsymbol{v}$, $D^{T}_{ij}(\boldsymbol{R})$ is the scale-dependent turbulent diffusion tensor, δ_{ij} is the Kronecker tensor, $I(\boldsymbol{R})$ is the source of particle number density fluctuations and $\langle ... \rangle$ denotes averaging over the statistics of turbulent velocity field and the Wiener process $\boldsymbol{w}(t)$. The Wiener trajectory $\boldsymbol{\xi}(t, \boldsymbol{x}|s)$ in the expressions for the turbulent diffusion tensor $D^{T}_{ij}(\boldsymbol{R})$ and other transport coefficients is defined as follows:

$$\boldsymbol{\xi}(t, \boldsymbol{x}|s) = \boldsymbol{x} - \int_s^t \boldsymbol{v}[\tau, \boldsymbol{\xi}(t, \boldsymbol{x}|\tau)]\; d\tau - \sqrt{2 D_m}\, \boldsymbol{w}(t - s), \tag{22}$$

where $\boldsymbol{w}(t)$ is the Wiener random process which describes the Brownian motion (molecular diffusion) and has the following properties: $\langle \boldsymbol{w}(t)\rangle_{\boldsymbol{w}} = 0$, $\langle w_i(t + \tau) w_j(t)\rangle_{\boldsymbol{w}} = \tau \delta_{ij}$, and $\langle \ldots \rangle_{\boldsymbol{w}}$ denotes the mathematical expectation over the statistics of the Wiener process. The velocity $v_i[\tau, \boldsymbol{\xi}(t, \boldsymbol{x}|\tau)]$ describes the Eulerian velocity calculated at the Wiener trajectory.

Equation (17) with $I(\boldsymbol{R}) = 0$ and for a delta-correlated in time random incompressible ($b = 0$) velocity field was derived by Kraichnan. [47] For a turbulent compressible flow with a finite correlation time Eq. (17) was derived using a stochastic calculus. [15] In particular, Wiener path integral representation of the solution of the Cauchy problem for Eq. (1), the Feynman-Kac formula and Cameron-Martin-Girsanov theorem were used for the derivation of Eq. (17). The comprehensive description of this method can be found also in Refs. 36, 37, and 48.

The source function $I(\boldsymbol{R})$ in Eq. (17) is related to the two source terms $-(\boldsymbol{v}{\cdot}\nabla)N - N\, \boldsymbol{\nabla}{\cdot}\, \boldsymbol{v}$ in the right hand side of Eq. (3), and the explicit expression for $I(\boldsymbol{R})$ is as follows (see Ref. 44):

$$I(\boldsymbol{R}) = B(\boldsymbol{R}) N^2 + \boldsymbol{U}^{(S)}(\boldsymbol{R}) \cdot \boldsymbol{\nabla} N^2 + \frac{3}{4} D^{T}_{ij}(\boldsymbol{R})\, (\nabla_i N)\, (\nabla_j N), \tag{23}$$

where $\boldsymbol{U}^{(S)}(\boldsymbol{R}) = (1/2)\left[\boldsymbol{U}(\boldsymbol{R}) + \boldsymbol{U}(-\boldsymbol{R})\right]$ and $\nabla_i^{(\boldsymbol{x})} \nabla_j^{(\boldsymbol{y})} N(t, \boldsymbol{x}) N(t, \boldsymbol{y}) = (3/4)\, (\nabla_i N)\, (\nabla_j N)$, and $\nabla_i \equiv \nabla_i^{(\boldsymbol{R})}$.

The meaning of the turbulent transport coefficients $B(\boldsymbol{R})$ and $\boldsymbol{U}(\boldsymbol{R})$ is as follows. The function $B(\boldsymbol{R})$ is determined by the compressibility of the particle velocity field. The vector $\boldsymbol{U}(\boldsymbol{R})$ determines a scale-dependent drift velocity which describes transport of fluctuations of particle number density from smaller scales to larger scales, i.e., in the regions with larger turbulent diffusion. The scale-dependent tensor of turbulent diffusion $D^{T}_{ij}(\boldsymbol{R})$ is equal to the tensor of the molecular (Brownian) diffusion in very small scales, while in the vicinity of the maximum scale of turbulent motions it coincides with the tensor of turbulent diffusion. It should be noticed also, that if $\boldsymbol{\nabla} N \neq 0$ a nonzero source term $I(\boldsymbol{R})$ causes the production of the particle number density fluctuations due to the tangling of the mean particle number density by the turbulent velocity field.

A. Degree of compressibility

If the turbulent velocity field is not delta-correlated in time (e.g., the correlation time is small yet finite), the tensor of turbulent diffusion, $D^{^{\rm T}}_{ij}(\boldsymbol{R})$, is compressible, i.e., $(\partial/\partial R_i) D^{^{\rm T}}_{ij}(\boldsymbol{R}) \neq 0$. The parameter $\sigma_{_T}$ that characterizes the degree of compressibility of the tensor of turbulent diffusion, is defined as follows:

$$\sigma_{_T} \equiv \frac{\nabla_i \nabla_j D^{\rm T}_{ij}(\boldsymbol{R})}{\nabla_i \nabla_j D^{\rm T}_{mn}(\boldsymbol{R}) \epsilon_{imp} \epsilon_{jnp}} \approx \frac{\langle (\boldsymbol{\nabla \cdot} \tilde{\boldsymbol{\xi}})^2 \rangle}{\langle (\boldsymbol{\nabla \times} \tilde{\boldsymbol{\xi}})^2 \rangle} \,, \qquad (24)$$

where ϵ_{ijk} is the fully antisymmetric Levi-Civita unit tensor, $\tilde{\boldsymbol{\xi}} = \boldsymbol{\xi} - \boldsymbol{x}$ with $|t-s| \gg \tau_0$. If the turbulent velocity field is a delta-correlated in time random process, then $\boldsymbol{\nabla \cdot} \tilde{\boldsymbol{\xi}} = -(\boldsymbol{\nabla \cdot v})\,(t-s)$, and $\boldsymbol{\nabla \times} \tilde{\boldsymbol{\xi}} = -(\boldsymbol{\nabla \times v})\,(t-s)$, and, hence, the expression for $\sigma_{_T}$ reads:

$$\sigma_{_T} = \frac{\langle (\boldsymbol{\nabla \cdot v})^2 \rangle}{\langle (\boldsymbol{\nabla \times v})^2 \rangle} \equiv \sigma_{\rm v}, \qquad (25)$$

where $\sigma_{\rm v}$ is the degree of compressibility of the particle velocity field. The parameter $\sigma_{\rm v}$ depends on the Stokes number [17]:

$$\sigma_{\rm v} = \frac{(8/3){\rm St}}{1 + \beta {\rm St}}, \qquad (26)$$

where the coefficient $\beta \sim 1$.

For small finite correlation time (i.e., for small Strouhal numbers, ${\rm Sr} = \tau_c \sqrt{\langle \boldsymbol{u}^2 \rangle}/\ell \ll 1$, the parameter $\sigma_{_T}$ can be estimated using Eq. (C12) in Ref. 15 (see also Ref. 44) as follows:

$$\sigma_{_T} = \sigma_{\rm v} + \frac{2\,{\rm Sr}^2}{3} \left(1 + \frac{913\,\sigma_{\rm v}^2}{12\,(1+\sigma_{\rm v})}\right) + O({\rm Sr}^4) \,. \qquad (27)$$

The mechanism of coupling related to the tangling of the gradient of the mean temperature gradient is quite robust. The properties of the tangling are not very sensitive to the exponent of the energy spectrum of the background turbulence. Anisotropy effects do not introduce new physics in the clustering process because the main contribution to the tangling clustering instability is at the Kolmogorov (viscous) scale of turbulent motions, where turbulence can be considered as nearly isotropic, while anisotropy effects can be essential in the vicinity of the maximum scales of the turbulent motions. Using these arguments, we consider the tensor $D^{^{\rm T}}_{ij}(\boldsymbol{R})$ for isotropic and homogeneous turbulent flow in the following form:

$$D^{^{\rm T}}_{ij}(\boldsymbol{R}) = D_{_{\rm T}} \biggl[[F(R) + F_c(R)] \delta_{ij} + R F_c' \frac{R_i R_j}{R^2} + \frac{R F'}{2} \left(\delta_{ij} - \frac{R_i R_j}{R^2} \right) \biggr], \qquad (28)$$

where $F(0) = 1 - F_c(0)$ and $F' = dF/dR$. The function $F_c(R)$ describes the compressible (potential) component, whereas $F(R)$ corresponds to vortical (incompressible) part of the turbulent diffusion tensor.

B. Derivation of expression for the function $B(\boldsymbol{R})$

Taking into account the equation of state of an ideal gas we obtain $p/P = \varrho/\rho + \theta/T + O(\varrho\theta/\rho T)$. For small Stokes numbers, $\boldsymbol{\nabla \cdot v} \approx (\tau_s/\rho)\, \boldsymbol{\nabla}^2 p$. This allows us to estimate $B(\boldsymbol{R})$ as

$$B(\boldsymbol{R}) \approx \frac{2\tau_s^2}{\rho^2} \, \langle \tau \bigl[\boldsymbol{\nabla}^2 p(\boldsymbol{x})\bigr] \, \bigl[\boldsymbol{\nabla}^2 p(\boldsymbol{y})\bigr] \rangle$$
$$\approx \frac{2\tau_s^2}{\rho^2} \, \frac{P^2}{T^2} \, \langle \tau \bigl[\boldsymbol{\nabla}^2 \theta(\boldsymbol{x})\bigr] \, \bigl[\boldsymbol{\nabla}^2 \theta(\boldsymbol{y})\bigr] \rangle, \qquad (29)$$

where $\boldsymbol{\nabla}^2 p(\boldsymbol{x}) = \bigl[\boldsymbol{\nabla}^{(\boldsymbol{x})}\bigr]^2 p(\boldsymbol{x})$, and we remind that the fluid density, temperature, and pressure have mean components, ρ, T, P, and fluctuations, ϱ, θ, p, respectively. Hereafter we omit the argument t in the correlation function. In $\boldsymbol{k}$ space the correlation function $\langle \tau \bigl[\boldsymbol{\nabla}^2 \theta(\boldsymbol{x})\bigr] \, \bigl[\boldsymbol{\nabla}^2 \theta(\boldsymbol{y})\bigr] \rangle$ reads:

$$\langle \tau \bigl[\boldsymbol{\nabla}^2 \theta(\boldsymbol{x})\bigr] \, \bigl[\boldsymbol{\nabla}^2 \theta(\boldsymbol{y})\bigr] \rangle = \int \tilde{\tau}(k)\, k^4 \, \langle \theta(\boldsymbol{k})\, \theta(-\boldsymbol{k}) \rangle \times \exp\bigl(i \boldsymbol{k \cdot R}\bigr)\, d\boldsymbol{k}. \qquad (30)$$

Taking into account that $\langle \theta(\boldsymbol{k})\, \theta(-\boldsymbol{k}) \rangle = \langle \theta^2 \rangle \tilde{E}_\theta(k)/4\pi k^2$, and integrating in $\boldsymbol{k}$ space we arrive to the following expressions for the functions $B(\boldsymbol{R})$:

$$B(\boldsymbol{R}) \approx \frac{2\,{\rm St}^2\, c_s^4}{3\,\tau_\eta\, u_0^4} \left(\frac{\ell_0 \boldsymbol{\nabla} T}{T}\right)^2 {\rm Re}^{1/2}, \qquad (31)$$

where $\tilde{E}_\theta(k) = (2/3)\, k_0^{-1}\, (k/k_0)^{-5/3}$ is the spectrum function of the temperature fluctuations for $k_0 \leq k \leq \ell_\eta^{-1}$, with $k_0 = \ell_0^{-1}$ and $\tilde{\tau}(k) = 2\tau_0\, (k/k_0)^{-2/3}$. To determine $\langle \theta^2 \rangle$ we used the budget equation for the temperature fluctuations $E_\theta = \langle \theta^2 \rangle/2$:

$$\frac{D E_\theta}{Dt} + {\rm div}\, \boldsymbol{\Phi}_\theta = -(\mathbf{F} \boldsymbol{\cdot} \boldsymbol{\nabla}) T - \varepsilon_\theta, \qquad (32)$$

which for homogeneous turbulence in a steady state yields:

$$\langle \theta^2 \rangle = -2\, \tau_0\, (\mathbf{F} \boldsymbol{\cdot} \boldsymbol{\nabla}) T = \frac{2}{3}\, (\ell_0 \boldsymbol{\nabla} T)^2 \,, \qquad (33)$$

where $F_i = \langle u_i \theta \rangle = -D^{(\theta)}_{_T} \nabla_i T$ is the turbulent heat flux, $D^{(\theta)}_{_T} = u_0 \ell_0/3$ is the turbulent diffusion of the temperature fluctuations and the dissipation rate of E_θ is $\varepsilon_\theta = \langle \theta^2 \rangle / 2\tau_0$ (see, e.g., Ref. 49).

On the other hand, the function $B(\boldsymbol{R})$ at very small scales has a universal form:

$$B(\boldsymbol{R}) = \frac{20\,\sigma_{\rm v}}{\tau_\eta\, (1 + \sigma_{\rm v})} \approx \frac{20\,\sigma_{\rm v}}{\tau_\eta} \approx \frac{160\,{\rm St}_{\rm eff}^2}{3\tau_\eta}, \qquad (34)$$

because at this scales the velocity field is smooth and nearly isotropic. Here we introduced the effective Stokes number using Eqs. (31) and (33):

$${\rm St}_{\rm eff} = {\rm St}\, \Gamma, \quad \Gamma({\rm Ma}, {\rm Re}, \ell_0/L_T) \approx \frac{{\rm Re}^{1/4}}{9\,{\rm Ma}^2} \left| \frac{\ell_0 \boldsymbol{\nabla} T}{T} \right|, \qquad (35)$$

where L_T is the characteristic scale of the mean temperature variations. To derive Eq. (34) we took into account that for a Gaussian velocity field [15]:

$$\langle (\boldsymbol{\nabla}\cdot\boldsymbol{v})^2\rangle = \frac{80}{3\,\tau_\eta^2}\,\mathrm{St}_{\rm eff}^2, \quad \langle (\boldsymbol{\nabla}\times\boldsymbol{v})^2\rangle = \frac{10}{\tau_\eta^2}. \tag{36}$$

Equation (36) yields:

$$\sigma_{\rm v} \equiv \frac{\langle (\boldsymbol{\nabla}\cdot\boldsymbol{v})^2\rangle}{\langle (\boldsymbol{\nabla}\times\boldsymbol{v})^2\rangle} = \frac{8}{3}\,\mathrm{St}_{\rm eff}^2 \ll 1. \tag{37}$$

Taking typical parameters for atmospheric turbulence $\mathrm{Re} = 10^7$, $u_0 = 1$ m/s and $\ell_0 = 100$ m with the temperature inversion, such that the mean temperature gradient, $|\boldsymbol{\nabla} T|$, is of the order of 1 K per 100 m, we obtain $\Gamma \approx 2.5\times 10^3$, or for $\mathrm{Re} = 10^6$, $u_0 = 0.3$ m/s and $\ell_0 = 30$ m the parameter Γ is $\Gamma \approx 5\times 10^3$.

IV. SOLUTION FOR TANGLING CLUSTERING INSTABILITY WITH $I = 0$

It is convenient to rewrite Eq. (17) for the two-point second-order correlation function $\Phi(R)$ in a non-dimensional form with coordinate R measured in units of the Kolmogorov scale, ℓ_η, time in units of the Kolmogorov time, τ_η and the function Φ in units of N^2:

$$\begin{aligned}\frac{\partial\Phi}{\partial t} &= \frac{1}{M(R)}\left[\Phi'' + 2\left(\frac{1}{R} + \chi(R)\right)\Phi'\right] + 2\tilde{U} R\,\Phi' \\ &\quad + B(R)\,\Phi + I(R), \end{aligned} \tag{38}$$

where

$$\begin{aligned}\frac{1}{M(R)} &= \frac{2}{\mathrm{Sc}} + \frac{2}{3}[1 - F - (RF_c)'], \\ \chi(R) &= -\frac{M(R)}{3}(F - 2F_c)', \qquad (39)\\ I(R) &= B(R) + \frac{4(\alpha-1)^2}{3}\,\left(\frac{\ell_0\boldsymbol{\nabla} T}{T}\right)^2 \\ &\quad\times\left(1 - \frac{3}{2M(R)} - \frac{R\,\chi(R)}{M(R)}\right), \qquad (40)\end{aligned}$$

$\mathrm{Sc} = \nu/D_m$ is the Schmidt number and $\boldsymbol{U} = \tilde{U}(R)\,\boldsymbol{R}$. Typically, in many applications, e.g., in the atmospheric turbulence, $\mathrm{Sc} \gg 1$ for small inertial particles. The two-point correlation function $\Phi(R)$ satisfies the following boundary conditions: $\Phi'(R=0) = 0$ and $\Phi(R\to\infty) = 0$. This function has a global maximum at $R = 0$ and therefore it satisfies the conditions:

$$\Phi''(R=0) < 0\,, \quad \Phi(R=0) > |\Phi(R>0)|\,.$$

For a steady-state regime and in the absence of the tangling clustering instability the solution of Eq. (38) was obtained in Ref. 44 for $I(R) \neq 0$. In this section we will consider solution of Eq. (38) for the case of the tangling clustering instability and $I(R) = 0$. Since the Schmidt number, $\mathrm{Sc} = \nu/D_m \gg 1$, the molecular diffusion scale is much less than the viscous Kolmogorov scale. This implies that the viscous range of scales essentially contributes to the tangling clustering instability. A general form of the turbulent diffusion tensor in the viscous range of scales is obtained taking into account that $F(R) = (1 - R^2)/(1 + \sigma_{_T})$ and $F_c(R) = \sigma_{_T}(1 - R^2)/(1 + \sigma_{_T})$, which yields:

$$D_{ij}^{\rm T}(\boldsymbol{R}) = C_1 R^2 \delta_{ij} + C_2 R_i R_j\,, \tag{41}$$

$$C_1 = \frac{2(2+\sigma_{_T})}{3(1+\sigma_{_T})}\,, \quad C_2 = \frac{2(2\sigma_{_T}-1)}{3(1+\sigma_{_T})}\,, \tag{42}$$

and the other functions in this range of scales are $\tilde{U} = 20\,\sigma_{\rm v}/3(1+\sigma_{\rm v})$ and $B = 20\,\sigma_{\rm v}/(1+\sigma_{\rm v})$.

In the *molecular diffusion range of scales*, $a_p/\ell_\eta \le R \le 1/\sqrt{\mathrm{Sc}}$, all terms $\propto R^2$ are small and can be neglected. Note that we consider the case when the particle radius, a_p, is the minimum scale of the problem, so that $a_p \le \ell_D$, where $\ell_D = \ell_0/\mathrm{Pe}^{3/4} = \ell_\eta/\sqrt{\mathrm{Sc}}$ is the molecular diffusion scale, and $\mathrm{Pe} = u_0\ell_0/D_m$ is the Peclet number. The solution of Eq. (38) in this range reads:

$$\Phi(R) = \left(1 - \frac{\mathrm{Sc}(B - \gamma\tau_\eta)}{12}R^2\right)\exp(\gamma t), \tag{43}$$

where $B > \gamma\tau_\eta$ and γ is the growth rate of the tangling clustering instability.

In the *turbulent diffusion region of scales*, $1/\sqrt{\mathrm{Sc}} \ll R \ll 1$, the molecular diffusion term $\propto 1/\mathrm{Sc}$ is negligible, and the solution of Eq. (38) in this region we seek for in the following form:

$$\Phi(R) \propto R^{-\beta}\exp(\gamma t). \tag{44}$$

Using the Corrsin integral, $\int_0^\infty R^2\Phi(R)\,dR = 0$, we obtain that $\beta = \lambda \pm i\kappa$ is a complex number, $\kappa^2 > 0$, where

$$\kappa^2 = \frac{4(B - \gamma\tau_\eta)(C_1 + C_2) - (C_1 - C_2 + 2\tilde{U})^2}{4(C_1 + C_2)^2}, \tag{45}$$

$$\begin{aligned}\lambda &= \frac{C_1 - C_2 + 2\tilde{U}}{2(C_1 + C_2)} = \frac{3 - \sigma_{_T}}{2(1 + 3\sigma_{_T})} \\ &\quad + \frac{10\sigma_{\rm v}}{1+\sigma_{\rm v}}\left(\frac{1+\sigma_{_T}}{1+3\sigma_{_T}}\right).\end{aligned} \tag{46}$$

Hence the real part of solution (44) is reduced to

$$\Phi(R) = C R^{-\lambda}\cos(\kappa\ln R + \varphi)\exp(\gamma t), \tag{47}$$

where C is the constant.

Since the correlation function $\Phi(R)$ has a global maximum in $R = a_p/\ell_\eta \ll 1$, the parameter $\sigma_T \le 3$. The function $\Phi(R)$ sharply decreases with the increase of R, for $R \gg 1$. The growth rate of the second moment of particles number density and the constant C can be obtained by matching the correlation function $\Phi(R)$ and its first derivative $\Phi'(R)$ at the boundaries of the above ranges, i.e., in the points $R = 1/\sqrt{\mathrm{Sc}}$ and $R = 1$. The matching yields $\kappa/2(C_1 + C_2) \approx \pi\, m/\ln\mathrm{Sc}$ (where $m = 2k+1$),

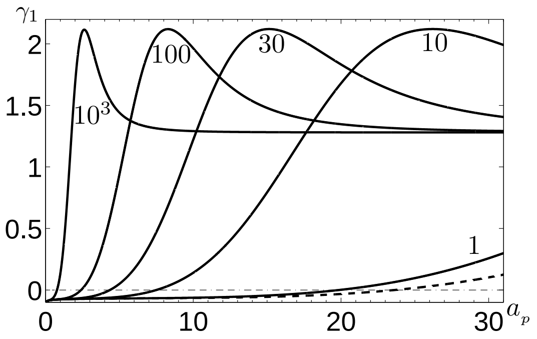

FIG. 1. The growth rate γ_1 of the tangling clustering instability (in units of $1/t_\eta$) of the first mode ($m = 1$) versus the particle radius a_p for different values of parameter Γ, and $\sigma_T = 1$, $\mathrm{Sc} = 10^6 a_p$. The particle radius a_p is given in μm. The dashed line corresponds to the inertial clustering instability.

and the growth rate for the mode $''m''$ of the tangling clustering instability is given by

$$\gamma_m = \frac{1}{3(1+3\sigma_T)}\biggl[\frac{200\sigma_{\rm v}(\sigma_T-\sigma_{\rm v})}{(1+\sigma_{\rm v})^2} - \frac{(3-\sigma_T)^2}{2(1+\sigma_T)} - \frac{2\pi^2 m^2(1+3\sigma_T)^2}{(1+\sigma_T)\ln^2\mathrm{Sc}}\biggr], \tag{48}$$

where $m = 1, 2, 3, \ldots$. The first mode ($m = 1$) has the minimum threshold for the excitation of the tangling clustering instability.

The tangling clustering instability depends on the ratio $\sigma_T/\sigma_{\rm v}$. For the δ-correlated in time random Gaussian compressible velocity field $\sigma_T = \sigma_{\rm v}$ (for details, see Refs. 15). In this case the second moment $\Phi(t, \boldsymbol{R})$ can only decay, in spite of the compressibility of the velocity field. On the contrary, for the finite correlation time of the turbulent velocity field $\sigma_T \neq \sigma_{\rm v}$, and the correlation function $\Phi(R)$ grows exponentially in time, i.e., the tangling clustering instability is excited.

Figures 1–2 show the growth rate (48) of the tangling clustering instability of the first mode ($m = 1$) versus the particle radius a_p for different values of parameter Γ. One can see from these figures that the characteristic time of the tangling clustering instability is of the order of the Kolmogorov time scale (the growth rate γ_1 in Figs. 1–2 is measured in units of the inverse Kolmogorov time). Remarkably that for every parameter $\Gamma(\mathrm{Re}, \mathrm{Ma})$ there is a rather sharp maximum of the function $\gamma_1(a_p)$. This implies that depending on the parameters of the turbulence there is a preferential particle size for which the particle clustering due to the tangling clustering instability is much faster than for other values of the particle size. Moreover, the growth rate of the tangling clustering instability is much larger than that of the inertial clustering instability (the growth rate for the inertial clustering instability in turbulence with a zero mean temperature gradient is shown in Fig. 1 by the dashed line).

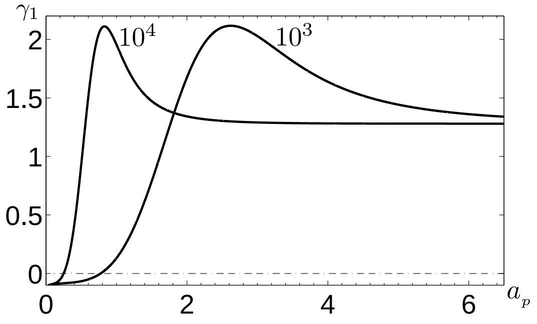

FIG. 2. The growth rate γ_1 of the tangling clustering instability of the first mode ($m = 1$) versus the particle radius a_p for larger values of parameter Γ, and $\sigma_T = 1$, $\mathrm{Sc} = 10^6 a_p$. The particle radius a_p is given in μm.

V. SOLUTION FOR TANGLING CLUSTERING INSTABILITY WITH $I \neq 0$

In this Section we obtain solution of Eq. (38) which includes both, the tangling clustering instability and the source term for the tangling clustering. This implies that we consider solution of Eq. (38) in the vicinity of the thresholds of the excitation of the tangling clustering instability.

Let us consider the *turbulent diffusion range of scales*, $1/\sqrt{\mathrm{Sc}} \ll R \ll 1$ and introduce the following function $\Psi(t, R) = \Phi(t, R)\, R^{1+\mu}$, where

$$\mu = \frac{1+\sigma_T}{1+3\sigma_T}\left(1 - 2\sigma_T + \frac{10\sigma_{\rm v}}{1+\sigma_{\rm v}}\right). \tag{49}$$

Equation (38) is reduced to the Schrodinger type equation:

$$\frac{\partial\Psi(t, R)}{\partial t} = \frac{1}{M(R)}\Psi'' - \mathcal{U}\,\Psi + I(R), \tag{50}$$

with the potential $\mathcal{U}$ and $1/M(R)$ in the form:

$$\mathcal{U} = -\frac{2}{3}\biggl[\frac{40\sigma_{\rm v}}{1+\sigma_{\rm v}}\left(1 + \frac{5\sigma_{\rm v}}{(1+\sigma_{\rm v})}\frac{(1+\sigma_T)}{(1+3\sigma_T)}\right) + (2\sigma_T - 1)\left(1 - (2\sigma_T - 1)\frac{1+\sigma_T}{1+3\sigma_T}\right)\biggr], \tag{51}$$

$$\frac{1}{M(R)} = \frac{2}{3}\frac{(1+3\sigma_T)}{(1+\sigma_T)}\,R^2, \quad I(R) = B\,R^{1+\mu}, \tag{52}$$

and $B = 20\sigma_{\rm v}/(1+\sigma_{\rm v})$. Here we took into account that the main contribution to the source term $I(R)$ for large Reynolds numbers is due to the first term $B(\boldsymbol{R})N^2$ in Eq. (23). Other contributions are negligible $\sim 10\mathrm{Re}^{-3/2}\ln^2\mathrm{Re}$ [see Eqs. (15) and (37)-(35)].

We choose the initial conditions which correspond to a turbulence without particle clusters: $\Psi(t = 0, R) =$

0. Now we seek a solution of Eq. (50) in the following form: $\Psi(t,R) = \sum_{m=1}^{\infty} f_m(t)\Psi_m(R)$ and $I(R) = B\sum_{m=1}^{\infty} A_m \Psi_m(R)$, where $\Psi_m(R)$ are the eigenfunctions determined by the following equation with $I(R)=0$:

$$\frac{1}{M(R)}\Psi_m'' - (\mathcal{U} + \gamma_m)\,\Psi_m = 0. \tag{53}$$

Concequently, the function $f_m(t)$ is determined by the following equation:

$$\frac{\partial f_m}{\partial t} = \gamma_m\, f_m + B\, A_m. \tag{54}$$

Taking into account the orthogonality of the eigenfunctions,

$$\frac{\int_0^\infty M(R)\Psi_m(R)\Psi_n(R)\,dR}{\int_0^\infty M(R)\Psi_m^2(R)\,dR} = \delta_{mn}, \tag{55}$$

and solving Eq. (54) we obtain the expressions for the function $f_m(t)$ and A_m:

$$f_m(t) = \frac{20\sigma_{\rm v}\, A_m}{(1+\sigma_{\rm v})\,\gamma_m}\,\left[\exp(\gamma_m t) - 1\right], \tag{56}$$

$$A_m = \frac{\int_0^\infty M(R) R^{1+\mu}\Psi_m(R)\,dR}{\int_0^\infty M(R)\Psi_m^2(R)\,dR}. \tag{57}$$

Taking into account that $\Phi_m(R = a_p) = \left[\Psi_m(t,R)\,R^{-(1+\mu)}\right]_{R=a_p} = 1$ we obtain the correlation function $\Phi(R=a_p,t)$ in the form:

$$\Phi(R=a_p,t) = \frac{20\sigma_{\rm v}}{1+\sigma_{\rm v}}\sum_{m=1}^{\infty}\frac{A_m}{\gamma_m}\left[\exp(\gamma_m t) - 1\right]. \tag{58}$$

When the tangling clustering instability is excited, it causes formation of a cluster with the particle number density inside the cluster, which is much larger than the mean particle number density.

The solution for $\Phi(t,R)$ [see Eq. (47)], which satisfies the above conditions has the following dimensional form:

$$\Phi(t,R) = N^2\,\frac{20\sigma_{\rm v}}{1+\sigma_{\rm v}}\sum_{m=1}^{\infty}\frac{A_m}{\gamma_m}\left(\frac{R}{\ell_D}\right)^{-\lambda}\cos\left[\kappa\ln\left(\frac{R}{\ell_D}\right)\right] \times\left[\exp(\gamma_m t) - 1\right]. \tag{59}$$

Here the correlation function $\Phi(t,R)$ has the global maximum at $R = \ell_D/\ell_\eta$, i.e., we assumed that in the molecular diffusion region the correlation function $\Phi(t,R)$ is nearly constant, $\Phi(t,R) \approx 1$ [see Eq. (43)]. The first minimum of the correlation function $\Phi(t,R)$ for the mode $m=1$ is located at $R = R_{\rm min} = \exp(1/\lambda)$, and it is given by

$$\frac{\Phi_{\rm min}}{N^2} = -\frac{B\,A_1\kappa}{e\,\gamma_1\,\lambda}\,{\rm Sc}^{-\lambda/2}\,\left[\exp(\gamma_1 t) - 1\right], \tag{60}$$

where we took into account that $\cos\left[\kappa\ln(R_{\rm min}/\ell_D)\right] = -\kappa/\lambda$. On the other hand, the maximum value of the correlation function $\Phi(t,R)$ is

$$\frac{\Phi_{\rm max}}{N^2} = \frac{B\,A_1}{\gamma_1}\,\left[\exp(\gamma_1 t) - 1\right], \tag{61}$$

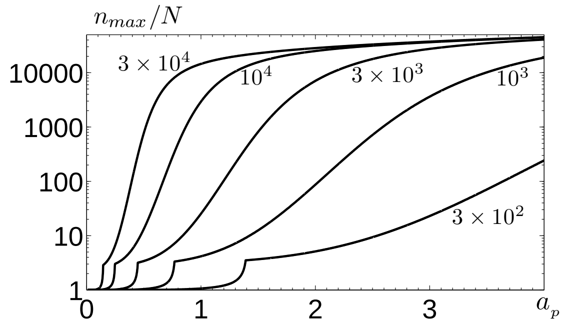

FIG. 3. The particle number density inside the cluster $n_{\rm max}/N$ versus the particle radius a_p for different values of parameter Γ, and $\sigma_{_T} = 1$, ${\rm Sc} = 10^6 a_p$. The particle radius a_p is given in μm.

where $\Phi_{\rm max} = \Phi(R=a_p,t)$ [see Eq. (58)]. This yields:

$$\frac{\Phi_{\rm min}}{\Phi_{\rm max}} = -\frac{\pi}{e\,\lambda}\left(\frac{{\rm Sc}^{-\lambda/2}}{\ln{\rm Sc}}\right). \tag{62}$$

Since $n_p = N + n \geq 0$, the function $\Phi(t,\boldsymbol{R}) \equiv \langle n(t,\boldsymbol{x})n(t,\boldsymbol{y})\rangle = \langle n_p(t,\boldsymbol{x})n_p(t,\boldsymbol{y})\rangle - N^2 \geq -N^2$. Therefore, the minimal possible value of the function $\Phi(t,\boldsymbol{R})$ is $\Phi_{\rm min} = -N^2$. This condition together with Eq. (62) allow us to estimate the maximum number density of particles attained inside the cluster during the tangling clustering instability:

$$\frac{n_p^{\rm max}}{N} = \left(1 + \frac{e\,\lambda}{\pi}\,{\rm Sc}^{\lambda/2}\,\ln{\rm Sc}\right)^{1/2}. \tag{63}$$

The maximum value of the particle number density inside the cluster, $n_{\rm max}/N$, versus the particle radius is shown in Fig. 3 for different values of parameter Γ. The discontinuity of the first derivative of $n_{\rm max}/N$ which is seen in Fig. 3 is related to the transition from one mechanism of particle tangling clustering due to the source term to another mechanism caused by the tangling clustering instability. The exponential growth at the linear stage of the instability is saturated by the nonlinear effects. The values of $n_{\rm max}/N$ in Fig. 3 are calculated using Eq. (63) that takes into account possible saturation of the tangling clustering instability caused by the exhaustion of the particles in the region surrounding the cluster. Inspection of Fig. 3 shows that the particle number density inside the cluster can increase in 10^4 times compared to the mean particle number density.

There are also other mechanisms leading to the nonlinear saturation of the tangling clustering instability discussed in detail in Ref. 15. However, as follows from our analysis the main significant mechanism of saturation of the growth of the tangling clustering instability for small particles is exhaustion of the particles in the surrounding area. Indeed, the tangling clustering instability causes strong redistribution of particles so that inside the clusters the particle number density is strongly increased at

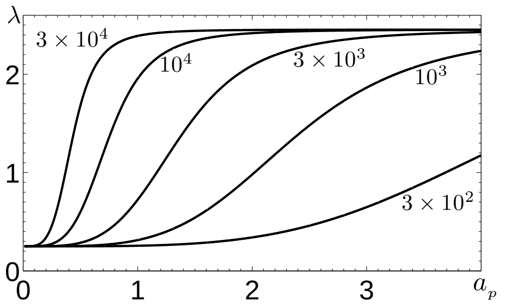

FIG. 4. The exponent λ versus the particle radius a_p for different values of parameter Γ and $\sigma_T = 1$. The particle radius a_p is given in μm.

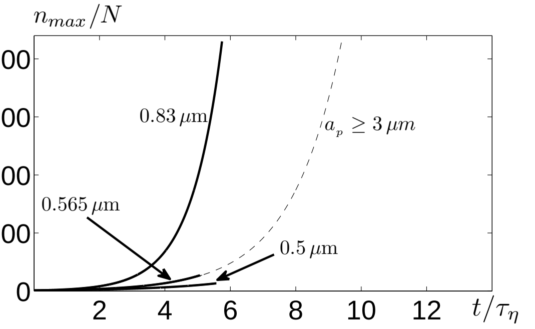

FIG. 5. The particle number density inside the cluster $n_{\rm max}/N$ as a function of time for different values of the particle radius a_p and $\Gamma = 10^4$, $\sigma_T = 1$, ${\rm Sc} = 10^6 a_p$. The particle radius a_p is given in μm. The dashed line is for $a_p \geq 3\mu$m.

some instant, while in surrounding regions it is essentially decreased. With the decrease of the number density of particles the hydrodynamic description becomes inapplicable. It should be noted that we consider situation when there is only the redistribution of the particles without their creation or annihilation. This implies that particles from the cluster vicinity are concentrated in the central part of it, which can be expressed using the Corrsin integral of the correlation function of the particle number density fluctuations: $\int_0^\infty \Phi(t,R) R^2\, dR = 0$. This condition implies that the tail of the correlation function $\Phi(t,R)$ must be negative [i.e., there is the anti-correlation tail of the function $\Phi(t,R)$]. The transition from central positive part $\Phi(t,R) > 0$ to the negative tail of $\Phi(t,R)$ occurs at the distance that is of the order of several Kolmogorov scales. Note, that in contrast to the inertial clustering, the tangling clustering instability accumulates particles into the cluster from the scales which are much larger than the Kolmogorov length scale. This is the reason why the concentration of particles inside the cluster increases due to the tangling clustering instability by several orders of magnitude.

The value $n_{\rm max}$ depends strongly on the Schmidt number Sc and on the exponent λ [see Eq. (63)]. The exponent λ depends on the degree of compressibility of the particle velocity field, $\sigma_{\rm v} \propto {\rm St}^2\, \Gamma({\rm Ma}, {\rm Re}, \ell_0/L_T)$ [see Eq. (35)]. The calculated values of exponent λ versus the particle radius for different values of parameter Γ are shown in Fig. 4, that explains strong dependence of the maximum particle number density inside the cluster $n_{\rm max}$ on the particle radius and the parameter Γ.

In general, other nonlinear mechanisms may limit the growth of the tangling clustering instability in the nonlinear stage of its evolution, and therefore they limit the maximum attainable value of the particle number density, $n_p^{\rm max}$, attained inside the cluster. For example, a momentum coupling of particles and turbulent fluid becomes essential when the mass loading parameter $\varsigma = m_{\rm p} n_{\rm max}/\rho$ is of the order of unity. [1] Introducing a mean particle mass density $\overline{\rho}_p = m_p\, N$ (e.g., in cloud physics it is a liquid water content measured in g/cm^3), we obtain the following constraint: $n_p^{\rm max}/N \leq \varsigma\rho/\overline{\rho}_p$. Using $\rho = 1.3 \times 10^{-3}$ g/cm^3 and $\overline{\rho}_p = 10^{-6}$ g/cm^3 we arrive at $n_p^{\rm max}/N \leq 1300$ for $\varsigma = 1$. This limiting effect should be taken into account together with the saturation mechanism caused by the exhaustion of the particles in the surrounding area of the cluster.

Figure 5 shows the temporal evolution of the number density of particles inside the cluster during the excitation of the tangling clustering instability for particles of different radius. Figure 5 reveals several interesting features pertinent to the instability, which deserve to be mentioned. The tangling clustering instability is less effective for very small particles, $a_p \leq 0.5\mu$m. The reason is that this instability is saturated by the exhaustion of the particles in the surrounding area of the cluster at a very low value $n_{\rm max}/N \approx 13.2$. For the particles having sub-micron and micron sizes the concentration inside the cluster can increase due to the tangling clustering instability up to several orders of magnitude. On the other hand, as follows from Fig. 2 the growth rate of the tangling clustering instability is the same for particles with $a_p = 0.565\mu$m and for all particles with $a_p \geq 3\mu$m. However, contrary to the case $a_p \geq 3\mu$m, the saturated value of the instability for $a_p = 0.565\mu$m is very low, $n_{\rm max}/N \approx 27.2$.

VI. EFFECT OF DROPLET EVAPORATION ON TANGLING CLUSTERING INSTABILITY

Let us study the effect of droplet evaporation on tangling clustering instability in stably stratified turbulence. The equation for the instantaneous number density $n_p(t,{\bf x})$ of droplets of the radius a_p is given by:

$$\frac{\partial n_p}{\partial t} + \nabla\cdot(n_p\, {\bf v}) = D_m\, \Delta n_p - \frac{n_p}{\tau_{\rm ev}} + I_0, \tag{64}$$

where the second term in the right hand part of Eq. (64) takes into account the droplet evaporation with the characteristic time $\tau_{\rm ev}$, and the last term, I_0, describes source of droplets due to condensation, which for simplicity is assumed to be constant. The equation for fluctuations of the droplet number density, $n(t,{\bf x}) = n_p(t,{\bf x}) - N(t,{\bf x})$, reads:

$$\frac{\partial n}{\partial t} + \nabla{\cdot}(n\,{\bf v} - \langle n\,{\bf v}\rangle) = D_m\,\Delta n - ({\bf v}{\cdot}\nabla)N - N\,\nabla{\cdot}\,{\bf v} \\ -\frac{n}{\tau_{\rm ev}}. \tag{65}$$

The last term in Eq. (65) describes the droplet evaporation. Using Eq. (65) we derive equation for the evolution of the two-point second-order correlation function of the droplet number density, $\Phi(t,{\bf R})$, see Eq. (17), in which

$$D_{ij}^{^T}({\bf R}) \approx 2\int_0^\infty \langle v_i\big[0,\boldsymbol{\xi}(t,{\bf x}|0)\big]\,v_j\big[\tau,\boldsymbol{\xi}(t,{\bf x}+{\bf R}|\tau)\big]\rangle \\ \times G(\tau)\,d\tau, \tag{66}$$

$$B({\bf R}) \approx 2\int_0^\infty \langle b\big[0,\boldsymbol{\xi}(t,{\bf x}|0)\big]\,b\big[\tau,\boldsymbol{\xi}(t,{\bf x}+{\bf R}|\tau)\big]\rangle \\ \times G(\tau)\,d\tau, \tag{67}$$

$$U_i({\bf R}) \approx -2\int_0^\infty \langle v_i\big[0,\boldsymbol{\xi}(t,{\bf x}|0)\big]\,b\big[\tau,\boldsymbol{\xi}(t,{\bf x}+{\bf R}|\tau)\big]\rangle \\ \times G(\tau)\,d\tau, \tag{68}$$

$G(\tau) = \exp(-\tau/\tau_{\rm ev})$, and other quantities are not changed by the droplet evaporation.

Equation for $\Phi(t,{\bf R})$ can be rewritten in a dimensionless form:

$$\frac{\partial\Phi}{\partial t} = \frac{1}{M(R)}\left[\Phi'' + 2\left(\frac{1}{R} + \chi(R)\right)\,\Phi'\right] \\ + \left[B(R) - \frac{2\tau_{_{\rm D}}}{\tau_{\rm ev}}\right]\,\Phi + I(R), \tag{69}$$

where distance R is measured in units of Kolmogorov scale ℓ_η and time t is measured in units of $\tau_\eta^2/\tau^{\rm eff} \equiv \tau_{_{\rm D}}/3$. Here the effective time $\tau^{\rm eff}$ is

$$\tau^{\rm eff} = \frac{\tau_\eta\tau_{\rm ev}}{\tau_\eta + \tau_{\rm ev}}, \tag{70}$$

a modified turbulent diffusion time is $\tau_{_{\rm D}} = \ell_\eta^2/D_{_{\rm T}}^{\rm eff}$, the effective turbulent diffusion coefficient $D_{_{\rm T}}^{\rm eff}$ in the Kolmogorov scale is given by [50]

$$D_{_{\rm T}}^{\rm eff} = \frac{\tau^{\rm eff}u_\eta^2}{3}, \tag{71}$$

and a modified function $1/M(R)$ is

$$\frac{1}{M(R)} = \frac{2}{\rm Sc^{\rm eff}} + \frac{2}{3}[1 - F - (RF_c)'], \tag{72}$$

where ${\rm Sc}^{\rm eff} = {\rm Sc}\,\tau^{\rm eff}/\tau_\eta$. Equation (69) shows that the evaporation decreases the source term $[B(R) - 2\tau_{_{\rm D}}/\tau_{\rm ev}]$ of the generation of fluctuations of the droplet number density.

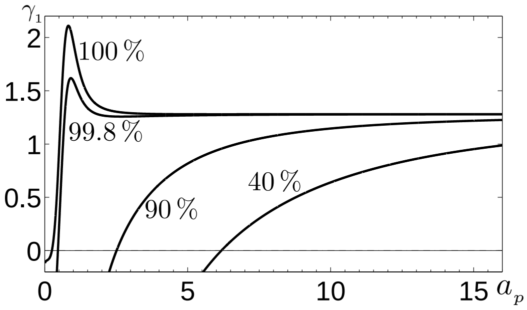

FIG. 6. The growth rate γ_1 of the tangling clustering instability (in units of $1/t_\eta$) of the first mode ($m = 1$) versus the particle radius a_p for different values of the relative humidity ϕ, and $\Gamma = 10^4$, $\sigma_{_T} = 1$, ${\rm Sc} = 10^6 a_p$. The particle radius a_p is given in μm. The dashed line corresponds to the inertial clustering instability.

The analysis similar to that performed in Sect. 4 yields the growth rate for the mode m of the tangling clustering instability:

$$\gamma_m = \frac{1}{3(1+3\sigma_{_T})}\left[\frac{200\sigma_{\rm v}(\sigma_{_T} - \sigma_{\rm v})}{(1+\sigma_{\rm v})^2} - \frac{(3-\sigma_{_T})^2}{2(1+\sigma_{_T})} \right. \\ \left. -\frac{2\pi^2 m^2(1+3\sigma_{_T})^2}{(1+\sigma_{_T})\ln^2 {\rm Sc}^{\rm eff}}\right] - \frac{2\tau_\eta^2}{\tau^{\rm eff}\tau^{\rm ev}}, \tag{73}$$

where $m = 1, 2, 3, \ldots$. This growth rate γ_m of the second moment of particles number density was obtained by matching the correlation function $\Phi(R)$ and its first derivative $\Phi'(R)$ at the points $R = 1/\sqrt{{\rm Sc}^{\rm eff}}$ and $R = 1$, which also yields: $\kappa/2(C_1 + C_2) \approx \pi\,m/\ln {\rm Sc}^{\rm eff}$. Therefore, the evaporation of droplets causes decrease of the instability growth rate. Figure 6 shows the growth rate γ_1 of the tangling clustering instability for different values of the relative humidity ϕ versus the particle radius. Here we used an expression for the evaporation time of droplets $\tau^{\rm ev} = 2.1\times 10^{-3}a_p^2/(1-\phi)$, where the droplet radius is in microns and time is in seconds (see, e.g., Ref. 51). As seen in Fig. 6, the evaporation of droplets drastically change the tangling clustering instability for small droplets, i.e., it increases the instability threshold in the droplet radius depending on the relative humidity ϕ. In addition, there is sharp maximum of the growth rate for 1 μm droplets if relative humidity is close to the supersaturated values: 99.8 % and 100 %. For low relative humidity the growth rate of the tangling clustering instability is less in comparison with the supersaturated case.

Figure 7 shows the temporal evolution of the number density of particles inside the cluster during the excitation of the tangling clustering instability for the relative humidity $\phi = 90\%$ and different droplet radius. This figure also demonstrates that the evaporation of droplets drastically change the tangling clustering instability.

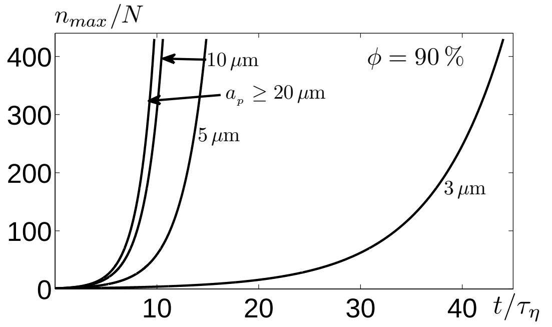

FIG. 7. The particle number density inside the cluster $n_{\rm max}/N$ as a function of time for different values of the particle radius a_p, and the relative humidity $\phi = 90\%$, $\Gamma = 10^4$, $\sigma_T = 1$, ${\rm Sc} = 10^6 a_p$. The particle radius a_p is given in μm.

VII. DISCUSSION AND CONCLUSIONS

The present study has been inspired by the previous work [44], where it was shown that the tangling clustering of inertial particles in the temperature stratified turbulence holds the potential to promote a strong clustering with the considerably enhanced particle concentration inside the cluster. Based on the thorough theoretical analysis, it is demonstrated in this study that the temperature fluctuations strongly contribute to the tangling clustering instability. Temperature fluctuations caused by tangling of the mean temperature gradient by the velocity fluctuations, produce pressure fluctuations and enhance considerably particle clustering. The growth rate of the tangling clustering instability is in $\sqrt{\rm Re}\,(\ell_0/L_T)^2/(3{\rm Ma})^4$ times larger than the growth rate of the inertial clustering instability.

The growth rate of the tangling clustering instability and the particle number density inside the cluster after saturation of the instability on the nonlinear stage depends on the parameter $\Gamma \approx \left({\rm Re}^{1/4}/9\,{\rm Ma}^2\right)\,\ell_0\,|\boldsymbol{\nabla} T|\,/T$. We also found that depending on the parameters of turbulence and the mean temperature gradient there is the preferential clustering of particles of a particular size (the growth rate of the tangling clustering instability has a sharp maximum at this size). We demonstrated the strong effect of the droplet evaporation on this instability. The tangling clustering instability in the temperature stratified turbulence may enhance significantly the collision rate of small particles, which is of interest for atmospheric physics and many other practical applications. In particular this effect can substantially accelerate the coalescence of small droplets in atmospheric turbulence with temperature gradients.

ACKNOWLEDGMENTS

This research was supported in part by the Israel Science Foundation governed by the Israeli Academy of Sciences (Grant 259/07), by EU COST Actions MP0806 and ES1004, by the EC FP7 project ERC PBL-PMES (Grant 227915), by the Russian Government Mega Grant (Grant 11.G34.31.0048), and by the Grant of Russian Ministry of Science and Education (Contract No. 8648).

---

[1] C. T. Crowe, J. D. Schwarzkopf, M. Sommerfeld and Y. Tsuji, *Multiphase flows with droplets and particles*, second edition (CRC Press LLC, NY, 2011).

[2] Z. Warhaft, “Passive scalars in turbulent flows,” Annu. Rev. Fluid Mech. **32**, 203 (2000).

[3] Z. Warhaft, “Laboratory studies of droplets in turbulence: towards understanding the formation of clouds,” Fluid Dyn. Res. **41**, 011201 (2009).

[4] S. Balachandar and J. K. Eaton, “Turbulent dispersed multiphase flow,” Annu. Rev. Fluid Mech. **42**, 111 (2010).

[5] R. Monchaux, M. Bourgoin, A. Cartellier, “Analyzing preferential concentration and clustering of inertial particles in turbulence,” Intern. J. Multiphase Flow **40**, 1 (2012).

[6] R. A. Shaw, “Particle-turbulence interactions in atmospheric clouds,” Annu. Rev. Fluid Mech. **35**, 183 (2003).

[7] R. E. Britter and S. R. Hanna, “Flow and dispersion in urban areas,” Annu. Rev. Fluid Mech. **35**, 469 (2003).

[8] A. Khain, M. Pinsky, T. Elperin, N. Kleeorin, I. Rogachevskii and A. Kostinski, “Critical comments to results of investigations of drop collisions in turbulent clouds,” Atmosph. Res. **86**, 1 (2007).

[9] H. Siebert, S. Gerashchenko, A. Gylfason, K. Lehmann, L. R. Collins, R. A. Shaw and Z. Warhaft, “Towards understanding the role of turbulence on droplets in clouds: In situ and laboratory measurements,” Atmosph. Res. **97**, 426 (2010).

[10] S. L. Post and J. Abraham, “Modeling the outcome of drop-drop collisions in Diesel sprays,” Int. J. Multiphase Flows **28**, 997 (2002).

[11] M. R. Maxey, “The gravitational settling of aerosol particles in homogeneous turbulence and random flow field,” J. Fluid Mech. **174**, 441 (1987).

[12] T. Elperin, N. Kleeorin, I. Rogachevskii, “Self-excitation of fluctuations of inertial particles concentration in turbulent fluid flow,” Phys. Rev. Lett. **77**, 5373 (1996).

[13] T. Elperin, N. Kleeorin, I. Rogachevskii, D. Sokoloff, “Turbulent transport of atmospheric aerosols and formation of large-scale structures,” Phys. Chem. Earth **A 25**, 797 (2000).

[14] E. Balkovsky, G. Falkovich and A. Fouxon, “Intermittent distribution of inertial particles in turbulent flows,” Phys. Rev. Lett. **86**, 2790 (2001).

[15] T. Elperin, N. Kleeorin, V. L’vov, I. Rogachevskii, D. Sokoloff, “Clustering instability of the spatial distribution of inertial particles in turbulent flows,” Phys. Rev. E **66**, 036302 (2002).

[16] B. Mehlig, M. Wilkinson, K. P. Duncan, T. Weber, M. Ljunggren, "On the aggregation of inertial particles in random flows," Phys. Rev. E **72**, 051104 (2005).

[17] T. Elperin, N. Kleeorin, M.A. Liberman, V.S. L'vov, I. Rogachevskii, "Clustering of aerosols in atmospheric turbulent flow," Environ. Fluid Mech. **7**, 173 (2007).

[18] P. Olla and R. M. Vuolo, "Concentration fluctuations of large Stokes number particles in a one-dimensional random velocity field," Phys. Rev. E **76**, 066315 (2007).

[19] I. Fouxon and P. Horvai, "Separation of Heavy Particles in Turbulence," Phys. Rev. Lett. **100**, 040601 (2008).

[20] P. Olla, "Preferential concentration versus clustering in inertial particle transport by random velocity fields," Phys. Rev. E **81**, 016305 (2010).

[21] G. Boffetta, F. De Lillo and A. Gamba, "Large scale inhomogeneity of inertial particles in turbulent flows," Phys. Fluids **16**, L20 (2003).

[22] L. R. Collins and A. Keswani, "Reynolds number scaling of particle clustering in turbulent aerosols," New J. Phys. **6**, 119 (2004).

[23] J. Chun, D. L. Koch, S. L. Rani, A. Ahluwalia and L. R. Collins, "Clustering of aerosol particles in isotropic turbulence," J. Fluid Mech. **536**, 219 (2005).

[24] L. Chen, S. Goto and J. C. Vassilicos, "Turbulent clustering of stagnation points and inertial particles," J. Fluid Mech. **553**, 143 (2006).

[25] H. Yoshimoto and S. Goto, "Self-similar clustering of inertial particles in homogeneous turbulence," J. Fluid. Mech. **577**, 275 (2007).

[26] J. Bec, L. Biferale, M. Cencini, A. Lanotte, S. Musacchio and F. Toschi, "Heavy particle concentration in turbulence at dissipative and inertial scales," Phys. Rev. Lett. **98**, 084502 (2007).

[27] M. van Aartrijk and H. J. H. Clercx, "Preferential concentration of heavy particles in stably stratified turbulence," Phys. Rev. Lett. **100**, 254501 (2008).

[28] J. Bec, L. Biferale, A. Lanotte, A. Scagliarini and F. Toschi, "Turbulent pair dispersion of inertial particles," J. Fluid Mech. **645**, 497 (2010).

[29] A. Aliseda, A. Cartellier, F. Hainaux and J. C. Lasheras, "Effect of preferential concentration on the settling velocity of heavy particles in homogeneous isotropic turbulence," J. Fluid Mech. **468**, 77 (2002).

[30] A. M. Wood, W. Hwang and J. K. Eaton, "Preferential concentration of particles in homogeneous and isotropic turbulence," Int. J. Multiphase Flow **31**, 1220 (2005).

[31] J. Salazar, J. de Jong, L. Cao, S. Woodward, H. Meng and L. Collins, "Experimental and numerical investigation of inertial particle clustering in isotropic turbulence," J. Fluid Mech. **600**, 245 (2008).

[32] H. Xu and E. Bodenschatz, "Motion of inertial particles with size larger than the Kolmogorov scale in turbulent flows," Physica D **237**, 2095 (2008).

[33] E. W. Saw, R. A. Shaw, S. Ayyalasomayajula, P. Y. Chuang and A. Gylfason, "Inertial clustering of particles in high Reynolds-number turbulence," Phys. Rev. Lett. **100** 214501 (2008).

[34] T. Elperin, N. Kleeorin and I. Rogachevskii, "Turbulent thermal diffusion of small inertial particles," Phys. Rev. Lett. **76**, 224 (1996).

[35] T. Elperin, N. Kleeorin and I. Rogachevskii, "Turbulent barodiffusion, turbulent thermal diffusion and large-scale instability in gases," Phys. Rev. E **55**, 2713 (1997).

[36] T. Elperin, N. Kleeorin, I. Rogachevskii and D. Sokoloff, "Passive scalar transport in a random flow with a finite renewal time: Mean-field equations," Phys. Rev. E **61**, 2617 (2000).

[37] T. Elperin, N. Kleeorin, I. Rogachevskii and D. Sokoloff, "Mean-field theory for a passive scalar advected by a turbulent velocity field with a random renewal time," Phys. Rev. E **64**, 026304 (2001).

[38] R. V. R. Pandya and F. Mashayek, "Turbulent thermal diffusion and barodiffusion of passive scalar and dispersed phase of particles in turbulent flows," Phys. Rev. Lett. **88**, 044501 (2002).

[39] M. W. Reeks, "On model equations for particle dispersion in inhomogeneous turbulence," Int. J. Multiph. Flow **31**, 93 (2005).

[40] M. Sofiev, V. Sofieva, T. Elperin, N. Kleeorin, I. Rogachevskii and S. S. Zilitinkevich, "Turbulent diffusion and turbulent thermal diffusion of aerosols in stratified atmospheric flows," J. Geophys. Res. **114**, D18209 (2009).

[41] N. E. L. Haugen, N. Kleeorin, I. Rogachevskii and A. Brandenburg, "Detection of turbulent thermal diffusion of particles in numerical simulations," Phys. Fluids **24**, 075106 (2012).

[42] J. Buchholz, A. Eidelman, T. Elperin, G. Grünefeld, N. Kleeorin, A. Krein, I. Rogachevskii, "Experimental study of turbulent thermal diffusion in oscillating grids turbulence," Experim. Fluids **36**, 879 (2004).

[43] A. Eidelman, T. Elperin, N. Kleeorin, I. Rogachevskii and I. Sapir-Katiraie, "Turbulent thermal diffusion in a multi-fan turbulence generator with the imposed mean temperature gradient," Experim. Fluids **40**, 744 (2006).

[44] A. Eidelman, T. Elperin, N. Kleeorin, B. Melnik and I. Rogachevskii, "Tangling clustering of inertial particles in stably stratified turbulence," Phys. Rev. E **81**, 056313 (2010).

[45] S. Chandrasekhar, "Stochastic problems in physics and astronomy," Rev. Modern Phys. **15**, 1 (1943).

[46] A. I. Akhiezer and S. V. Peletminsky, *Methods of Statistical Physics* (Pergamon, Oxford, 1981).

[47] R. H. Kraichnan, "Small-scale structure of a scalar field convected by turbulence," Phys. Fluids **11**, 945 (1968).

[48] Ya. B. Zeldovich, A. A. Ruzmaikin, and D. D. Sokoloff, *The Almighty Chance* (Word Scientific Publ., Singapore, 1990), and references therein.

[49] S. S. Zilitinkevich, T. Elperin, N. Kleeorin and I. Rogachevskii, "Energy- and flux budget (EFB) turbulence closure model for stably stratified flows. Part I: Steady-state, homogeneous regimes," Boundary-Layer Meteorol. **125**, 167 (2007).

[50] T. Elperin, N. Kleeorin and I. Rogachevskii, "Effect of chemical reactions and phase transitions on turbulent transport of particles and gases," Phys. Rev. Lett. **80**, 69 (1998).

[51] J. H. Seinfeld and S. N. Pandis, *Atmospheric Chemistry and Physics. From Air Pollution to Climate Change.*, 2nd ed. (John Wiley & Sons, NY, 2006).